

# Collision-Induced Dissociation Studies of $\text{Co}(\text{CO})_x^+$ , $x = 1-5$ : Sequential Bond Energies and the Heat of Formation of $\text{Co}(\text{CO})_4$

Susanne Goebel,<sup>†</sup> Chris L. Haynes, Farooq A. Khan,<sup>‡</sup> and P. B. Armentrout\*

Contribution from the Department of Chemistry, University of Utah, Salt Lake City, Utah 84112

Received March 13, 1995<sup>Ⓢ</sup>

**Abstract:** Sequential bond dissociation energies of  $\text{Co}(\text{CO})_x^+$  ( $x = 1-5$ ) have been determined in collision-induced dissociation (CID) experiments with Xe using guided-ion beam mass spectrometry. Analysis of the CID thresholds provides the following 0 K bond dissociation energies:  $D_0[(\text{CO})_4\text{Co}^+-\text{CO}] = 0.78 \pm 0.05$  eV,  $D_0[(\text{CO})_3\text{Co}^+-\text{CO}] = 0.78 \pm 0.06$  eV,  $D_0[(\text{CO})_2\text{Co}^+-\text{CO}] = 0.85 \pm 0.12$  eV,  $D_0[(\text{CO})\text{Co}^+-\text{CO}] = 1.58 \pm 0.09$  eV, and  $D_0[\text{Co}^+-\text{CO}] = 1.80 \pm 0.07$  eV. The ligand exchange reaction of  $\text{CoCO}^+ + \text{Xe}$  provides a  $\text{Co}^+-\text{Xe}$  bond energy,  $D_0(\text{Co}^+-\text{Xe}) = 0.80 \pm 0.14$  eV, consistent with a previous determination. The values here, along with the established heats of formation for  $\text{Co}^+$  and CO and the ionization energy of  $\text{Co}(\text{CO})_4$ , indicate that the 298 K heat of formation of  $\text{Co}(\text{CO})_4^+$  is  $256 \pm 18$  kJ/mol and that of  $\text{Co}(\text{CO})_4$  is  $-551 \pm 20$  kJ/mol. The latter value can be used to determine that  $D_{298}[(\text{CO})_4\text{Co}-\text{Co}(\text{CO})_4] = 83 \pm 29$  kJ/mol. The trends in the sequential cobalt carbonyl bond energies are compared with those of other metals and discussed in terms of the electronic structure of the complexes.

## Introduction

Transition metals and transition metal complexes are important catalysts for industrial applications and for organic synthesis.<sup>1-3</sup> Fundamental studies designed to elucidate the mechanisms of such chemistry often point to unsaturated organometallic complexes as key intermediates, but there is little accurate information about the thermodynamics of such species. Gas-phase chemistry offers the opportunity to investigate such complexes and it also has the advantage of removing solvent effects, thereby providing intrinsic thermodynamic values. In previous work from this laboratory, guided-ion beam mass spectrometry has been used to study the carbonyl cations of iron,<sup>4</sup> chromium,<sup>5</sup> and nickel<sup>6</sup> systems, where the neutral monometal carbonyl species are stable, 18-electron species; vanadium,<sup>7</sup> where the neutral is stable but a 17-electron complex; and copper and silver<sup>8</sup> systems, where the neutral carbonyl complexes are unknown. In the present work, we extend these studies to the cobalt carbonyl cations, a system where the stable neutral carbonyl involves two metal centers in order to satisfy the 18-electron rule,  $\text{Co}_2(\text{CO})_8$ . Thus, the cobalt carbonyl cations,  $\text{Co}(\text{CO})_x^+$  ( $x = 1-5$ ), are interesting because they are isoelectronic with the  $\text{Fe}(\text{CO})_x$  ( $x = 1-5$ ) neutral

complexes. These experiments are designed to provide direct thermodynamic information on these species and to provide insight into the electronic structure of metal carbonyls.

## Literature Thermochemistry

A number of ionization studies have been carried out on various cobalt carbonyl species,  $\text{XCo}(\text{CO})_4$  where  $\text{X} = \text{Co}(\text{CO})_4$ ,<sup>9-11</sup> H,<sup>12</sup>  $\text{SiY}_3$  ( $\text{Y} = \text{F}, \text{CH}_3, \text{Cl}$ ),<sup>13-15</sup> and NO.<sup>16,17</sup> Bond dissociation energies for the cobalt carbonyl cations,  $D[(\text{CO})_{x-1}\text{Co}^+-\text{CO}]$ , can be obtained from these studies as the difference in appearance energies of  $\text{Co}(\text{CO})_x^+$  and  $\text{Co}(\text{CO})_{x-1}^+$ . These values are collected in Table 1 and can be seen to vary considerably from molecule to molecule. We attribute this to the difficulty of accurately measuring the true appearance energy for reactions that involve considerable dissociation, processes that tend to be affected by kinetic shifts. The only other experimental thermochemistry comes from a kinetic energy release distribution (KERD) experiment on  $\text{Co}^+(\text{acetone}-d_6)$  eliminating ethane- $d_6$ .<sup>18</sup> In this study by Hanratty et al., a bond dissociation energy of  $D_0[\text{Co}^+-\text{CO}] = 1.34 \pm 0.13$  eV was obtained, but a recent reanalysis of these data provides a value of  $1.70 \pm 0.13$  eV.<sup>19</sup> *Ab initio* calculations, which include a

<sup>†</sup> Present address: Technische Universitat Braunschweig, Department of Chemistry, Braunschweig D-38106, Germany.

<sup>‡</sup> Present address: Department of Chemistry, West Georgia College, Carrollton, GA 30118.

<sup>Ⓢ</sup> Abstract published in *Advance ACS Abstracts*, June 15, 1995.

(1) See, for example: Cotton, F. A.; Wilkinson, G. *Advanced Inorganic Chemistry*, 5th ed.; Wiley: New York, 1988. Huheey, J. E. *Inorganic Chemistry: Principles of Structure and Reactivity*, 3rd ed.; Harper and Row: New York, 1983.

(2) Hoffmann, R. *Angew. Chem., Int. Ed. Engl.* **1982**, *21*, 711.

(3) Wender, I.; Pino, P., Eds. *Organic Syntheses via Metal Carbonyls*; Wiley: New York, 1968.

(4) Schultz, R. H.; Crellin, K. C.; Armentrout, P. B. *J. Am. Chem. Soc.* **1991**, *113*, 8590.

(5) Khan, F. A.; Clemmer, D. E.; Schultz, R. H.; Armentrout, P. B. *J. Phys. Chem.* **1993**, *97*, 7978.

(6) Khan, F. A.; Steele, D. L.; Armentrout, P. B. *J. Phys. Chem.* **1995**, *99*, 7819.

(7) Sievers, M. R.; Armentrout, P. B. *J. Phys. Chem.* **1995**, *99*, 8135.

(8) Meyer, F.; Chen, Y.-M.; Armentrout, P. B. *J. Am. Chem. Soc.* **1995**, *117*, 4071.

(9) Winters R. E.; Kiser, R. W. *J. Phys. Chem.* **1965**, *69*, 1618.

(10) Bidinosti, D. R.; McIntyre, N. S. *J. Chem. Soc., Chem. Commun.* **1967**, 1.

(11) Bidinosti, D. R.; McIntyre, N. S. *Can. J. Chem.* **1970**, *48*, 593.

(12) Saalfeld, F. E.; McDowell, M. V.; Gondal, S. K.; MacDiarmid, A. G. *J. Am. Chem. Soc.* **1968**, *90*, 3684.

(13) Saalfeld, F. E.; McDowell, M. V.; Hagen, A. P.; MacDiarmid, A. G. *Inorg. Chem.* **1968**, *7*, 1665.

(14) Saalfeld, F. E.; McDowell, M. V.; Gondal, S. K.; MacDiarmid, A. G. *Inorg. Chem.* **1968**, *7*, 1465.

(15) Saalfeld, F. E.; McDowell, M. V.; MacDiarmid, A. G. *J. Am. Chem. Soc.* **1970**, *92*, 2324.

(16) Foffani, A.; Pignataro, S.; Distefano, G.; Innorta, G. *J. Organomet. Chem.* **1967**, *7*, 473.

(17) Lloyd, D. R.; Schlag, E. W. *Inorg. Chem.* **1969**, *8*, 2544.

(18) Hanratty, M. A.; Beauchamp, J. L.; Illies, A. J.; van Koppen P.; Bowers, M. T. *J. Am. Chem. Soc.* **1988**, *110*, 1.

(19) Carpenter, C. J.; van Koppen, P. A. M.; Bowers, M. T. *J. Am. Chem. Soc.* Submitted for publication.

**Table 1.** Summary of values for  $D[(\text{CO})_{x-1}\text{Co}^+-\text{CO}]$  (eV)

reference	$x = 1$	$x = 2$	$x = 3$	$x = 4$	$x = 5$
Winters and Kiser <sup>a</sup>	$2.5 \pm 0.6$	$1.7 \pm 0.6$	$1.8 \pm 0.5$	$1.0 \pm 0.5^b$	
Saalfeld et al. <sup>c</sup>	2.8, 2.3, 2.9, $1.9 \pm 0.5$	2.1, 1.5, $1.7 \pm 0.5$	0.8, $1.9 \pm 0.5$		
Saalfeld et al. <sup>d</sup>	$1.9 \pm 0.3$	$1.9 \pm 0.3$			
Saalfeld et al. <sup>e</sup>	$3.1 \pm 0.5$	$1.7 \pm 0.5$			
Carpenter et al. <sup>f</sup>	$1.70 \pm 0.13^g$				
Barnes et al. <sup>h</sup>	$1.55^i$ [1.62] <sup>j</sup>	$1.31^i$ [1.40] <sup>j</sup>			
this work <sup>s</sup>	$1.80 \pm 0.07$	$1.58 \pm 0.09$	$0.85 \pm 0.12$	$0.78 \pm 0.06$	$0.78 \pm 0.05$

<sup>a</sup> Reference 9. <sup>b</sup> Although the normalized ion current for  $\text{Co}(\text{CO})_4^+$  is shown in this reference, no appearance potential was reported. The value given here is an estimate based on Figure 1 in this reference. <sup>c</sup> Reference 12. <sup>d</sup> Reference 13. <sup>e</sup> Reference 14. <sup>f</sup> Reference 19. <sup>g</sup> 0 K values. <sup>h</sup> Reference 20. <sup>i</sup>  $D_e$  values.

**Table 2.** Literature Thermochemistry (kJ/mol)<sup>a</sup>

species	$\Delta_f H_0^\circ$	$\Delta_f H_{298}^\circ$
CO	$-113.81 \pm 0.17$	$-110.53 \pm 0.17$
Co	$425.1 \pm 2.1$	$426.7 \pm 2.1$
$\text{Co}^+$	$1183.5 \pm 6.3^b$	$1191.2 \pm 6.3^b$
$\text{Co}(\text{CO})_4$	$-566 \pm 12$	$-561 \pm 12^c$
	$-556 \pm 20^{d,e}$	$-551 \pm 20^{d,e}$
$\text{Co}(\text{CO})_4^+$	$235 \pm 15^d$	$246 \pm 15^d$
	$245 \pm 18^e$	$256 \pm 18^e$
$\text{Co}_2(\text{CO})_8$		$-1185.4 \pm 6.0^f$

<sup>a</sup> All species are in the gaseous state. Unless otherwise stated, all data in this table are taken from ref 28. Ion heats of formation at 298.15 K correspond to the thermal electron convention. <sup>b</sup> Calculated by using  $\text{IE}(\text{Co}) = 7.86 \pm 0.06$  eV taken from ref 42. <sup>c</sup> References 23 and 24. <sup>d</sup> Calculated by using  $\text{IE}[\text{Co}(\text{CO})_4] = 8.3 \pm 0.1$  eV, ref 10. <sup>e</sup> This work. See text. <sup>f</sup> Reference 22.

relativistic correction, by Barnes et al.<sup>20</sup> find values of  $D_e[\text{Co}^+-\text{CO}] = 1.62$  eV and  $D_e[(\text{CO})\text{Co}^+-\text{CO}] = 1.40$  eV.

Also of interest in this work is the thermochemistry of the  $\text{Co}(\text{CO})_4$  radical. Winters and Kiser<sup>9</sup> recommended a heat of formation for this species of  $-552$  kJ/mol based on their measurement of the appearance energy (AE) of  $16.9 \pm 0.4$  eV for dissociative ionization of  $\text{Co}_2(\text{CO})_8$  to form  $\text{Co}^+ + 4\text{CO} + \text{Co}(\text{CO})_4$ . This was based on an estimated  $\Delta_f H^\circ[\text{Co}_2(\text{CO})_8]$  value of  $-1423$  kJ/mol, and led to a bond energy of 318 kJ/mol for  $D[(\text{CO})_4\text{Co}-\text{Co}(\text{CO})_4]$ . If a more recent value for  $\Delta_f H_{298}^\circ[\text{Co}_2(\text{CO})_8]$ ,  $-1185.4 \pm 6.0$  kJ/mol,<sup>21,22</sup> is used with information from Table 2, then this AE yields  $\Delta_f H_{298}^\circ[\text{Co}(\text{CO})_4] = -304 \pm 40$  kJ/mol and  $D[(\text{CO})_4\text{Co}-\text{Co}(\text{CO})_4] = 578 \pm 56$  kJ/mol. This value is certainly incorrect and indicates that the AE value is undoubtedly shifted to higher energies or does not correspond to production of  $\text{Co}(\text{CO})_4$ .

Bidinosti and McIntyre<sup>10</sup> obtained a different value for this bond energy by measuring the AE of  $\text{Co}(\text{CO})_4^+$  from  $\text{Co}_2(\text{CO})_8$ ,  $8.8 \pm 0.1$  eV, and the ionization energy (IE) of the  $\text{Co}(\text{CO})_4$  radical,  $8.3 \pm 0.1$  eV. The difference between these two values,  $0.5 \pm 0.2$  eV =  $48 \pm 19$  kJ/mol, equals  $D_0[(\text{CO})_4\text{Co}-\text{Co}(\text{CO})_4]$ , much lower than the value of Winters and Kiser. They attributed this discrepancy to the inaccuracy of the estimated heat of formation of  $\text{Co}_2(\text{CO})_8$ , the difficulty of accurately measuring the appearance energy for the  $\text{Co}^+$  ion in the Winters and Kiser study, and the possibility of competing processes. Bidinosti and McIntyre also examined the temperature dependence of the  $\text{Co}_2(\text{CO})_8 = 2\text{Co}(\text{CO})_4$  equilibrium over a range of 333 to 383 K to determine a bond energy of  $61 \pm 8$  kJ/mol. They estimate that the 0 K value should be about  $54 \pm 13$  kJ/mol.

Pilcher,<sup>23</sup> Connor,<sup>24</sup> and Pilcher and Skinner<sup>22</sup> all cite Bidinosti and McIntyre's results and use  $\Delta_f H_{298}^\circ[\text{Co}(\text{CO})_4] = -561 \pm 12$  kJ/mol. These works cite different  $D_{298}[(\text{CO})_4\text{Co}-\text{Co}(\text{CO})_4]$  bond energies (92, 68, and 87.8 kJ/mol, respectively), in part because the heat of formation of  $\text{Co}_2(\text{CO})_8$  was continually refined. Pilcher and Skinner<sup>22,23</sup> obtain their values by determining a mean cobalt-carbonyl disruption enthalpy, and combining that with the heats of formation for  $\text{Co}_2(\text{CO})_8$  and  $\text{Co}_4(\text{CO})_{12}$  and the effect of bridging carbonyls. In their critical compilation of organometallic thermochemistry, Simoes and Beauchamp<sup>25</sup> use  $D[(\text{CO})_4\text{Co}-\text{Co}(\text{CO})_4] = 64$  kJ/mol, citing Connor<sup>24</sup> and Skinner and Pilcher.<sup>22</sup> This value can be obtained from the heats of formation,  $\Delta_f H_{298}^\circ[\text{Co}_2(\text{CO})_8] = -1185.4 \pm 6.0$  kJ/mol<sup>22</sup> and  $\Delta_f H_{298}^\circ[\text{Co}(\text{CO})_4] = -561 \pm 12$  kJ/mol,<sup>24</sup> indicating that the bond energy has an uncertainty of  $\pm 18$  kJ/mol. Lastly, Folga and Ziegler use density functional theory to calculate  $D[(\text{CO})_4\text{Co}-\text{Co}(\text{CO})_4] = 148.0$  kJ/mol,<sup>26</sup> which is substantially larger than the more reliable experimental values.

Combining  $\Delta_f H_{298}^\circ[\text{Co}(\text{CO})_4] = -561 \pm 12$  kJ/mol with  $\text{IE}[\text{Co}(\text{CO})_4] = 8.3 \pm 0.1$  eV leads to  $\Delta_f H_{298}^\circ[\text{Co}(\text{CO})_4^+] = 246 \pm 20$  kJ/mol in the thermal electron convention. Based on this thermochemistry and the other literature information in Table 2, the sum of the four bonds in the  $\text{Co}(\text{CO})_4^+$  complex at 298 K is  $503 \pm 21$  kJ/mol ( $5.21 \pm 0.22$  eV).

In order to compare the literature values to the results measured here, we need to convert our thermodynamic data between temperatures of 298.15 and 0 K. The heat of formation of a compound at 0 K can be derived by using the following relationship for polyatomic molecules:

$$\Delta_f H_0^\circ - \Delta_f H_{298}^\circ = [H_0^\circ - H_{298}^\circ]_{\text{compound}} - \sum [H_0^\circ - H_{298}^\circ]_{\text{elements}} \quad (1)$$

where for a nonlinear polyatomic molecule

$$[H_0^\circ - H_T^\circ]_{\text{compound}} \approx -4RT - RT \sum u_i (e^{-u_i} - 1) \quad (2)$$

and  $u = hv_i/k_B T$ . The  $4RT$  term in eq 2 has contributions of  $3RT/2$  from translation,  $3RT/2$  from rotation, and  $RT$  from  $\Delta PV = \Delta nRT$  for 1 mol of ideal gas. The summation in eq 2 is carried out over the vibrational frequencies of the polyatomic molecule,  $\nu_i$ . No vibrational frequencies for  $\text{Co}(\text{CO})_4$  have been determined, so we use frequencies of  $\text{Fe}(\text{CO})_4^+$  taken from Ricca et al.<sup>27</sup> and listed in Table 3 for  $\text{Co}(\text{CO})_4^+$ . They calculate that there are two low-lying states, a high-spin tetrahedral complex and a low-spin square planar complex, so we use the

(20) Barnes, L. A.; Rosi, M.; Bauschlicher, C. W. *J. Chem. Phys.* **1990**, *93*, 609.

(21) Gardner, P. J.; Cartner, A.; Cunningham, R. G.; Robinson, B. H. *J. Chem. Soc., Dalton Trans.* **1975**, 2582.

(22) Pilcher, G.; Skinner, H. A. *The Chemistry of the Metal-Carbon Bond*; Hartley, F. R., Patai, S., Eds.; Wiley: New York, 1982; p 43.

(23) Pilcher, G. *Thermochemistry and Thermodynamics*; Phys. Chem. Series 2, Vol. 10; Int. Rev. Sci., Butterworths: London, 1975; Chapter 2, p 45.

(24) Connor, J. A. *Top. Curr. Chem.* **1977**, *71*, 71.

(25) Simoes, J. A. M.; Beauchamp, J. L. *Chem. Rev.* **1990**, *90*, 629.

(26) Folga, E.; Ziegler, T. *J. Am. Chem. Soc.* **1993**, *115*, 5169.

(27) Ricca, A.; Bauschlicher, C. W., Jr. *J. Phys. Chem.* **1994**, *98*, 12899.

**Table 3.** Vibrational Frequencies and Average Internal Energies

species	$E_{\text{int}}^a$	vibrational frequencies (cm <sup>-1</sup> ) <sup>b</sup>
CoCO <sup>+</sup>	0.0297	319(2), 423, 2225
Co(CO) <sub>2</sub> <sup>+</sup>	0.0995	81(2), 289(2), 348, 400, 441(2), 2217, 2268
Co(CO) <sub>3</sub> <sup>+</sup>	0.1680	61(2), 71, 255(2), 276, 293, 306(2), 354(2), 372, 2222(2), 2267
Co(CO) <sub>4</sub> <sup>+</sup>	0.2429	A: <sup>c</sup> 55(2), 73(3), 258(3), 275, 304(3), 351(2), 377(3), 2226(3), 2269
	0.2020	B: <sup>d</sup> 49, 95, 96(2), 102, 315(2), 335, 345, 357, 386(2), 443, 540, 546, 584(2), 2201(2), 2219, 2262
Co(CO) <sub>5</sub> <sup>+</sup>	0.2691	48, 78(2), 96, 101(2), 108, 312(2), 316, 335, 340, 357, 385(2), 416, 465(2), 533, 568, 584(2), 2201(2), 2206, 2215, 2258

<sup>a</sup> Average internal vibrational energy at 300 K. <sup>b</sup> Vibrational frequencies taken from ref 27. Degeneracies are shown in parentheses. <sup>c</sup>  $T_d$  symmetry. <sup>d</sup>  $D_{4h}$  symmetry.

average of both to estimate the vibrational contribution to the enthalpy change,  $(-8.66 \pm 0.80)RT$ . This means that  $[H_0^\circ - H_{298}^\circ]$  for Co(CO)<sub>4</sub> is  $(-12.66 \pm 0.80)RT = -31.37 \pm 2.0$  kJ/mol. The enthalpy changes,  $[H_0^\circ - H_{298}^\circ]$ , of the elements are  $-4.771$ ,  $-4.204$ , and  $-17.366$  kJ/mol for Co(c), 4C-(graphite) and 2O<sub>2</sub>, respectively.<sup>28</sup> From eq 1, these values yield  $\Delta_f H_0^\circ - \Delta_f H_{298}^\circ$  for Co(CO)<sub>4</sub>(g) and Co(CO)<sub>4</sub><sup>+</sup>(g) of  $-5.0 \pm 2.0$  and  $-11.23 \pm 2.0$  kJ/mol, respectively. These give the 0 K heats of formation for Co(CO)<sub>4</sub> and Co(CO)<sub>4</sub><sup>+</sup> listed in Table 1. The latter value leads to a sum of bond energies at 0 K of  $493 \pm 17$  kJ/mol ( $5.11 \pm 0.17$  eV) for Co(CO)<sub>4</sub><sup>+</sup>.

To compare individual bond energies measured here with those determined in the literature, we also need to convert from 0 to 298 K bond dissociation energies (BDEs). Following the method outlined above, we determine that the BDEs for (CO)<sub>x-1</sub>-Co<sup>+</sup>-CO at 298 K are larger than those at 0 K by 3.41, 1.94, 0.81, 5.41 (if  $D_{4h}$  symmetry; 1.44 if  $T_d$  symmetry), and 2.19 (if Co(CO)<sub>4</sub> is  $D_{4h}$  symmetry; 6.17 if it is  $T_d$  symmetry) kJ/mol for  $x = 1-5$ , respectively. The vibrational frequencies needed for this calculation are listed in Table 3 and are assumed to equal those calculated by Ricca et al. for Fe(CO)<sub>x</sub><sup>+</sup>.<sup>27</sup>

## Experimental Section

The guided-ion beam instrument on which these experiments were performed has been described in detail previously.<sup>29,30</sup> Ions are created in a flow tube source as described below, extracted from the source, accelerated, and passed through a magnetic sector for mass analysis. The mass-selected ions are decelerated to the desired kinetic energy and focused into an octopole beam guide.<sup>29</sup> This device uses radio-frequency electric fields to trap the ions in the radial direction and ensure complete collection of reactant and product ions. The octopole passes through a gas cell of effective length 8.26 cm that contains the neutral collision partner at relatively low pressures (0.05–0.3 mTorr). The unreacted parent and product ions drift to the end of the octopole, from which they are extracted, passed through a quadrupole mass filter for mass analysis, and detected with a secondary electron scintillation ion detector using standard pulse counting techniques. Raw ion intensities are converted to cross sections as described previously.<sup>29</sup> We estimate absolute cross sections to be accurate to  $\pm 20\%$ .

Laboratory (lab) energies are converted to energies in the center of mass (CM) frame by using the conversion  $E_{\text{CM}} = E_{\text{lab}}M/(M + m)$ , where  $m$  and  $M$  are the ion and neutral masses, respectively. The absolute energy scale and corresponding full width at half maximum (fwhm) of the ion beam kinetic energy distribution are determined by using the octopole as a retarding energy analyzer as described previously.<sup>29</sup> The absolute uncertainty in the energy scale is  $\pm 0.05$  eV (lab). The energy distributions are nearly Gaussian and have a typical fwhm of 0.2–0.5 eV (lab).

**Ion Source.** Co(CO)<sub>x</sub><sup>+</sup> ( $x = 1-5$ ) ions are made in our flow tube source, described in detail previously.<sup>30</sup> Co<sup>+</sup> ions are produced by using a direct current discharge source<sup>4</sup> consisting of a cobalt cathode held at a high negative voltage (1.5–3 kV) over which a flow of

approximately 90% He and 10% Ar passes at room temperature. Ar<sup>+</sup> ions created in the discharge are accelerated toward the cobalt cathode, sputtering off ionic and neutral metal atoms. CO gas is added to the flow about 60 cm downstream of the discharge. (If this gas is added too close to the discharge or if a high pressure is used, ionized CO clusters are formed. Because the masses of the (CO)<sub>x+2</sub><sup>+</sup> clusters are only 3 amu below those of the Co(CO)<sub>x</sub><sup>+</sup> ions, this can create potential problems in initial mass selection of the ions.) Co(CO)<sub>x</sub><sup>+</sup> ions are then formed by three-body collisions. At typical flow tube pressures of 0.5–0.6 Torr, the ions undergo  $> 10^4$  thermalizing collisions as they traverse the remaining 40 cm of the flow tube. Ions are extracted from the flow tube and gently focused through a 9.5 cm long differentially pumped region before entering the rest of the instrument described above.

For all of the cobalt carbonyl complex ions, except for CoCO<sup>+</sup>, there were indications of excited states formed by this procedure. We have previously found that adding approximately 1–3 mTorr of methane (in this study, upstream of the point where CO is added) will quench excited states of Co<sup>+</sup>.<sup>31</sup> The efficiency of this cooling was verified by a comparison of flow tube results with and without methane added. The CID cross sections in the CoCO<sup>+</sup> + Xe reaction system were not influenced by addition of methane. In all other systems, Co(CO)<sub>x</sub><sup>+</sup> ( $x = 2-5$ ), there were cooling effects observed when methane was added to the flow tube. Only those data for Co(CO)<sub>x</sub><sup>+</sup> ( $x = 2-5$ ) where methane is added to quench excited states were analyzed for thermochemistry as described below.

**Thermochemical Analysis.** Cross sections are modeled by using eq 3,<sup>4,32</sup>

$$\sigma = \sigma_0 \sum_i g_i (E + E_i + E_{\text{rot}} - E_0)^n / E \quad (3)$$

where  $E$  is the relative translational energy,  $E_0$  is the reaction threshold at 0 K,  $E_{\text{rot}}$  is the average rotational energy [ $0.039$  eV =  $3k_B T/2$ ,  $T = 300$  K for Co(CO)<sub>x</sub><sup>+</sup> ( $x = 3-5$ ) and  $0.026$  eV =  $k_B T$  for CoCO<sup>+</sup> and Co(CO)<sub>2</sub><sup>+</sup>] of the reactant ions,  $\sigma_0$  is an energy-independent scaling parameter, and the exponent  $n$  is treated as a variable parameter. Vibrational energies of the polyatomic reactants are included explicitly as a summation over vibrational energy levels,  $i$ , with energies  $E_i$  and relative populations  $g_i$  ( $\sum_i g_i = 1$ ). We use the Beyer–Swinehart algorithm<sup>33</sup> to calculate a Maxwell–Boltzmann distribution of vibrational energies at 300 K which is used for the factors  $g_i$  in eq 3. We have described this modeling procedure in detail elsewhere.<sup>4</sup> The vibrational frequencies needed for this analysis are shown in Table 3 and are assumed to equal those of Fe(CO)<sub>x</sub><sup>+</sup> calculated by Ricca et al.<sup>27</sup> In the case of Co(CO)<sub>4</sub><sup>+</sup> where two geometries were calculated, analysis was performed with both sets of frequencies.

## Results

Collision-induced dissociation (CID) of Co(CO)<sub>x</sub><sup>+</sup> species results in the sequential elimination of the CO molecules as the energy is increased. This is apparent in the data for Co(CO)<sub>5</sub><sup>+</sup>, shown in Figure 1, which is typical of the CID results for all the cobalt carbonyl cations. No ions with different numbers of C and O atoms are observed. This observation is

(28) Chase, M. W., Jr.; Davies, C. A.; Downey, J. R., Jr.; Frurip, D. J.; McDonald, R. A.; Syverud, A. N. *J. Phys. Chem. Ref. Data* **1985**, *14*, Suppl. No. 1 (JANAF Tables).

(29) Ervin, K. M.; Armentrout, P. B. *J. Chem. Phys.* **1985**, *83*, 166.

(30) Schultz, R. H.; Armentrout, P. B. *Int. J. Mass Spectrom. Ion Processes* **1991**, *107*, 29.

(31) Haynes, C. L.; Armentrout, P. B. *Organometallics* **1994**, *13*, 3480.

(32) Armentrout, P. B. In *Advances in Gas Phase Ion Chemistry*; Adams, N. G., Babcock, L. M., Eds.; JAI: Greenwich, 1992; Vol. 1, p 83.

(33) Beyer, T.; Swinehart, D. F. *Commun. ACM* **1973**, *16*, 379.

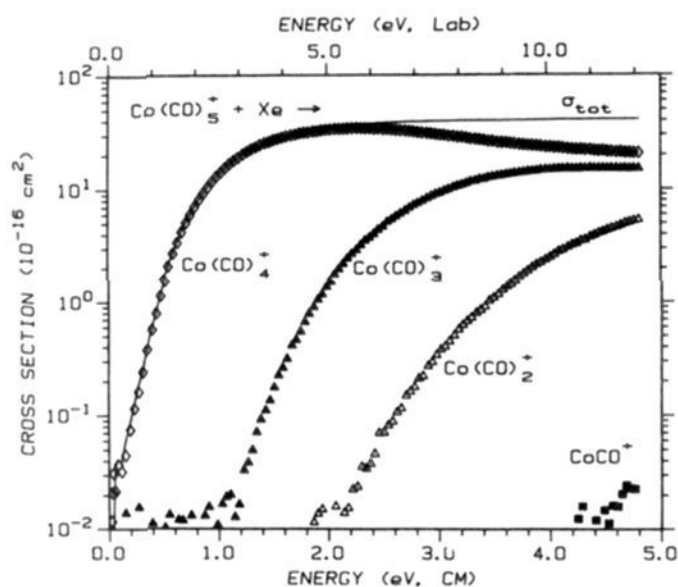


**Figure 1.** Cross sections for reaction of  $\text{Co}(\text{CO})_5^+$  with Xe as a function of relative kinetic energy (lower  $x$  axis) and laboratory energy (upper  $x$  axis) at a xenon pressure of 0.05 mTorr. Sequential loss of CO ligands occurs to form  $\text{Co}(\text{CO})_4^+$ ,  $\text{Co}(\text{CO})_3^+$ ,  $\text{Co}(\text{CO})_2^+$ , and  $\text{CoCO}^+$ . The solid line shows the total cross section.

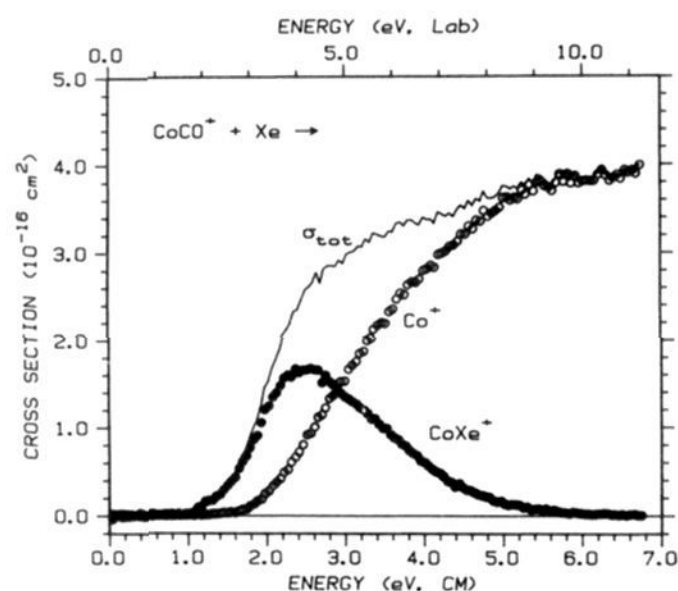


**Figure 2.** Cross sections for reaction of  $\text{CoCO}^+$  with Xe as a function of relative kinetic energy (lower  $x$  axis) and laboratory energy (upper  $x$  axis) at a xenon pressure of 0.05 mTorr. The solid line shows the total cross section.

easily rationalized because an individual CO bond is substantially stronger than even the sum of the metal ligand bonds in  $\text{Co}(\text{CO})_5^+$ .

Other than CID, the only other process observed in this study is the ligand exchange reaction 4.



Ligand exchange is probably taking place with  $\text{Co}(\text{CO})_x^+$  ( $x \geq 2$ ) as well; however, we did not measure the cross sections for these products, most of which are too massive to be analyzed in our quadrupole mass filter.

Effects due to multiple collisions with Xe were examined by performing the experiments at two or three different Xe gas cell pressures (0.05, 0.2, 0.3 mTorr). All systems studied here show slight, for  $\text{CoCO}^+$ , to moderate pressure affects, for  $\text{Co}(\text{CO})_x^+$  ( $x = 2-5$ ). The data shown in Figures 1–6 correspond to low-pressure conditions (0.05 mTorr).

**CID of  $\text{Co}(\text{CO})_x^+$ .** In this section, we examine the variations in the CID behavior of the five cobalt carbonyl cations. The interaction of  $\text{CoCO}^+$  with Xe is shown in Figure 2. The two products observed are  $\text{Co}^+$  and  $\text{CoXe}^+$ . The cross section for  $\text{Co}^+$  has an apparent threshold of  $\sim 1.6$  eV. Ligand exchange to form  $\text{CoXe}^+$  exhibits a lower apparent threshold (near 1 eV) and has a cross section that peaks as the cross section for the CID process increases. The mass resolution of the quadrupole

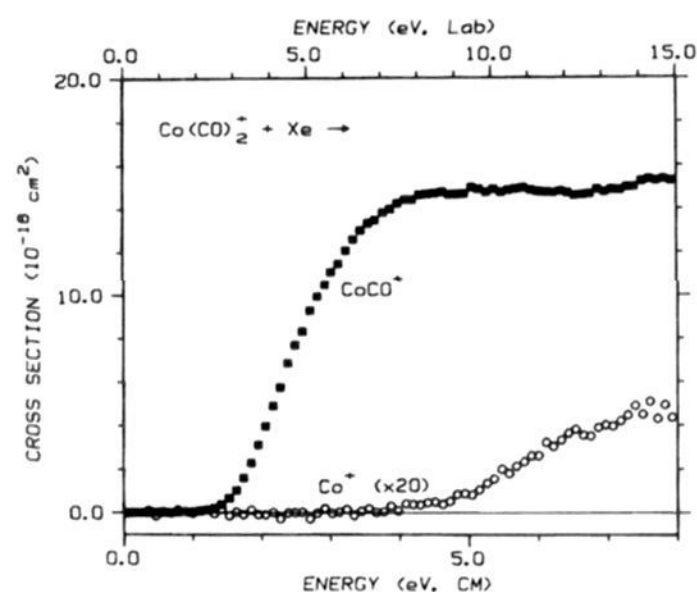


**Figure 3.** Cross sections for reaction of  $\text{Co}(\text{CO})_2^+$  with Xe as a function of relative kinetic energy (lower  $x$  axis) and laboratory energy (upper  $x$  axis) at a xenon pressure of 0.05 mTorr. The  $\text{Co}^+$  cross section is multiplied by a factor of 20.

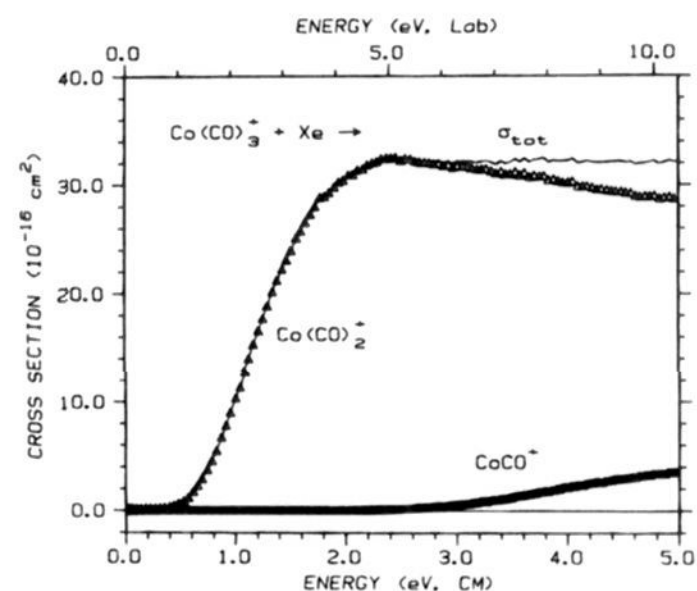


**Figure 4.** Cross sections for reaction of  $\text{Co}(\text{CO})_3^+$  with Xe as a function of relative kinetic energy (lower  $x$  axis) and energy in the laboratory frame (upper  $x$  axis) at a xenon pressure of 0.05 mTorr. The solid line shows the total cross section.

mass spectrometer was set sufficiently low that the cross section shown in Figure 2 should represent the product intensities for all isotopes of Xe.

Results for the CID of  $\text{Co}(\text{CO})_2^+$  with Xe are shown in Figure 3. The cross section for  $\text{CoCO}^+$  has a somewhat lower apparent threshold than that for formation of  $\text{Co}^+$  in Figure 2. Loss of two CO ligands from  $\text{Co}(\text{CO})_2^+$  is very inefficient and rises from an apparent threshold of about 4 eV.

The CID pattern in  $\text{Co}(\text{CO})_3^+$ , shown in Figure 4, is different from that of  $\text{CoCO}^+$  and  $\text{Co}(\text{CO})_2^+$  in that the apparent threshold for the loss of a single CO is substantially lower and the cross section is much larger. This cross section declines somewhat at the apparent threshold for the formation of  $\text{CoCO}^+$ , showing that CO molecules are eliminated sequentially with increasing energy. Again, the loss of two CO ligands from  $\text{Co}(\text{CO})_3^+$  is inefficient, but much more efficient than in the  $\text{Co}(\text{CO})_2^+$  case.

The CID pattern for  $\text{Co}(\text{CO})_4^+$  is illustrated in Figure 5. The threshold for the loss of a single CO is similar to that for the loss of one CO ligand in the CID reaction of  $\text{Co}(\text{CO})_3^+$ . The  $\text{Co}(\text{CO})_3^+$  cross section exhibits an appreciable decline at the apparent onset of  $\text{Co}(\text{CO})_2^+$ . This behavior is clearly due to the sequential nature of CO loss because the total cross section remains fairly constant at elevated energies, Figure 5.

Figures 1 and 6 illustrate the CID results of  $\text{Co}(\text{CO})_5^+$ . The major product channel is the loss of one CO ligand to form  $\text{Co}(\text{CO})_4^+$ . The apparent threshold for this process is similar

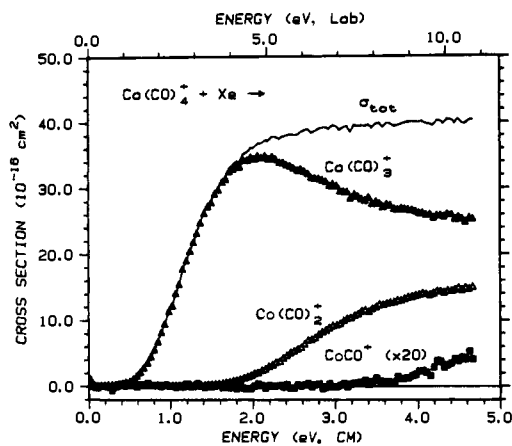


**Figure 5.** Cross sections for reaction of  $\text{Co}(\text{CO})_4^+$  with Xe as a function of relative kinetic energy (lower  $x$  axis) and laboratory energy (upper  $x$  axis) at a xenon pressure of 0.05 mTorr. The solid line shows the total cross section. The  $\text{CoCO}^+$  cross section is multiplied by a factor of 20.

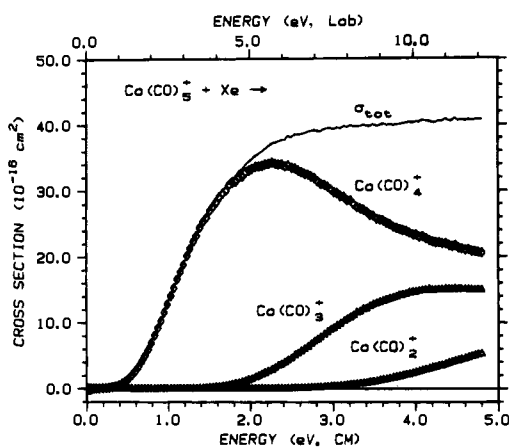
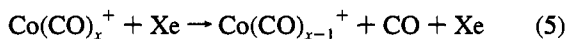


**Figure 6.** Cross sections for reaction of  $\text{Co}(\text{CO})_5^+$  with Xe as a function of relative kinetic energy (lower  $x$  axis) and laboratory energy (upper  $x$  axis) at a xenon pressure of 0.05 mTorr. The solid line shows the total cross section. The  $\text{CoCO}^+$  product is not shown due to its extremely small cross section magnitude.

to the thresholds for loss of one CO ligand in the CID reactions of  $\text{Co}(\text{CO})_4^+$  and  $\text{Co}(\text{CO})_3^+$ . Additional CO ligands are lost from the primary  $\text{Co}(\text{CO})_4^+$  product as the energy is raised to form  $\text{Co}(\text{CO})_3^+$ ,  $\text{Co}(\text{CO})_2^+$ , and  $\text{CoCO}^+$ . For this complex, the CID reaction is still quite efficient for the loss of two or even three CO ligands. At energies  $> 1$  eV, the primary cross section starts to decline due to the competition with secondary and tertiary products channels. This is verified by looking at the total cross section,  $\sigma_{\text{tot}}$ , which remains fairly constant at higher kinetic energies.

**BDEs from Primary Thresholds.** Bond dissociation energies for  $\text{Co}(\text{CO})_x^+$  ions can be obtained from threshold analysis of the primary dissociation channels, reaction 5,



and from the differences between the thresholds for sequential CO ligand loss. In previous CID experiments,<sup>4-6</sup> we concluded that the primary thresholds provided the most accurate thermochemical information because they are least susceptible to kinetic shifts. Consistent with this, we found it more difficult in the present study to accurately model the secondary reactions. In addition, data for the primary product ions are extrapolated to zero pressure before analysis, although consistent results are also obtained for the lowest pressure data (0.05 mTorr). For

**Table 4.** Parameters Used in Eq 3

species	$\sigma_0$	$n$	$E_0$ (eV) <sup>a</sup>	$E_0$ (prim) <sup>b</sup>
<b>CoCO<sup>+</sup> + Xe</b>				
$\text{Co}^+$	$2.5 \pm 0.5$	$1.6 \pm 0.2$	$1.80 \pm 0.07$	
$\text{CoXe}^+$	$1.6 \pm 0.6$	$2.6 \pm 0.5$	$1.00 \pm 0.12$	
<b>Co(CO)<sub>2</sub><sup>+</sup> + Xe</b>				
$\text{CoCO}^+$	$15.9 \pm 1.7$	$1.7 \pm 0.3$	$1.58 \pm 0.09$	
$\text{Co}^+$	$0.05 \pm 0.04$	$2.2 \pm 0.4$	$3.23 \pm 0.25$	$3.38 \pm 0.11$
<b>Co(CO)<sub>3</sub><sup>+</sup> + Xe</b>				
$\text{Co}(\text{CO})_2^+$	$47.3 \pm 2.7$	$1.6 \pm 0.3$	$0.85 \pm 0.12$	
$\text{CoCO}^+$	$2.4 \pm 0.9$	$2.1 \pm 0.4$	$2.41 \pm 0.20$	$2.43 \pm 0.15$
<b>Co(CO)<sub>4</sub><sup>+</sup> + Xe</b>				
$\text{Co}(\text{CO})_3^+$	$48.0 \pm 2.2$	$2.1 \pm 0.3$	$0.78 \pm 0.06^{\text{d}}$	
	$47.8 \pm 1.6$	$2.1 \pm 0.3$	$0.81 \pm 0.08^{\text{e}}$	
$\text{Co}(\text{CO})_2^+$	$12.9 \pm 3.0$	$2.3 \pm 0.4$	$1.79 \pm 0.11$	$1.63 \pm 0.13$
<b>Co(CO)<sub>5</sub><sup>+</sup> + Xe</b>				
$\text{Co}(\text{CO})_4^+$	$44.1 \pm 0.9$	$1.6 \pm 0.2$	$0.78 \pm 0.05^{\text{c}}$	
	$45.6 \pm 2.5$	$1.6 \pm 0.3$	$0.86 \pm 0.09$	
$\text{Co}(\text{CO})_3^+$	$7.3 \pm 2.3$	$2.9 \pm 0.5$	$1.67 \pm 0.12$	$1.56 \pm 0.08$
$\text{Co}(\text{CO})_2^+$	$1.7 \pm 0.4$	$3.0 \pm 0.2$	$2.57 \pm 0.09$	$2.41 \pm 0.14$

<sup>a</sup> Uncertainties in parentheses. No RRKM analysis is included unless otherwise noted. <sup>b</sup> Calculated using experimental values from primary thresholds. <sup>c</sup> Analysis with RRKM included. <sup>d</sup> The average of the thresholds obtained from the  $T_d$  ( $0.81 \pm 0.07$  eV) and  $D_{4h}$  ( $0.75 \pm 0.05$  eV) geometries. <sup>e</sup> The average of the thresholds obtained from the  $T_d$  ( $0.86 \pm 0.08$  eV) and  $D_{4h}$  ( $0.77 \pm 0.06$  eV) geometries.

data on the secondary and tertiary product ions, we analyze only the lowest pressure data (0.05 mTorr).

Listed in Table 4 are the optimized parameters of eq 3 obtained from the analyses of reaction 5 for between three and five independent data sets for all ions. In the case of  $\text{CoCO}^+$ , only data sets where no  $\text{CH}_4$  was present in the flow tube were analyzed as there was no effect observed upon addition of  $\text{CH}_4$ . For all the other species, we analyzed only data sets where methane was present in the flow tube to quench excited state ions. For  $\text{Co}(\text{CO})_4^+$  and  $\text{Co}(\text{CO})_5^+$ , RRKM analysis of the lifetime of the dissociating ion was included, as described elsewhere.<sup>5</sup> This analysis explicitly examines lifetime effects on the thresholds, which accounts for ions with energy in excess of the dissociation energy that do not dissociate within our experimental time window of  $\sim 10^{-4}$  s. As can be seen in Table 4, an effect is observed in the cases of  $\text{Co}(\text{CO})_4^+$  and  $\text{Co}(\text{CO})_5^+$ , although it is small, 0.03 and 0.08 eV, respectively. We also verified that this effect was negligible for the  $\text{Co}(\text{CO})_3^+$ , and presume this to be true for  $\text{Co}(\text{CO})_2^+$  and  $\text{CoCO}^+$ . The vibrational frequencies estimated for the transition states for  $\text{Co}(\text{CO})_4^+$  and  $\text{Co}(\text{CO})_5^+$  dissociation are chosen as discussed in detail elsewhere.<sup>5</sup> Briefly, we take frequencies for the  $\text{Co}(\text{CO})_x^+$  reactant minus a Co-CO stretch as the reaction coordinate, replacing a CO stretch by the frequency for free CO, and dividing the frequencies for four transitional modes (bends, wags and/or twists) by a factor of 2.

Before comparison with the experimental data, the model cross section of eq 3 (or its form that incorporates lifetime effects)<sup>5</sup> is convoluted over the ion and neutral translational energy distributions, as described previously.<sup>29</sup> The parameters in eq 3,  $\sigma_0$ ,  $E_0$ , and  $n$ , are then optimized by using a nonlinear least-squares analysis to best reproduce the data. From all of the acceptable fits of independent data sets, mean values for  $\sigma_0$ ,  $E_0$ , and  $n$  are obtained. Uncertainties in the reported thresholds are derived from the spread of  $E_0$  values in different data sets acquired in experimental runs on two to four different days, from a  $\pm 20\%$  variation in the vibrational frequencies listed for the  $\text{Co}(\text{CO})_x^+$  ions and the transition states when the RRKM analysis is included, from the absolute error in the energy scale,



and from a factor of 2 variation of the time window in the lifetime analysis.

Because the vibrational, rotational, and translational energy distributions of the reactants are explicitly included in our modeling, the thresholds obtained correspond to 0 K values. We also take these thresholds to equal  $D_0[(\text{CO})_{x-1}\text{Co}^+-\text{CO}]$ , implicitly assuming that there are no activation barriers in excess of endothermicity for dissociation. Based on theoretical considerations,<sup>34</sup> the long-range ion-induced dipole and ion-dipole attraction, and a kinetic energy release distribution study on the decomposition of  $\text{Mn}(\text{CO})_x^+$ ,<sup>35</sup> this is a reasonable assumption for metal carbonyl species and one that leads to accurate BDEs for other metal carbonyl systems studied previously.<sup>4-8</sup> In addition, for all but one of the complexes studied here, there are no electronic considerations that might lead to dissociation to excited state asymptotes, as discussed in more detail below. Also discussed below is evidence that the dissociation energy probably corresponds to the adiabatic value for the single exception.

One possible complexity in the accurate determination of BDEs by CID methods is whether the ligand exchange reactions of  $\text{Co}(\text{CO})_x^+$  with Xe, e.g. reaction 4, might cause a competitive shift in the observed thresholds, especially if cross sections for the ligand exchange processes are large or the  $\text{Co}(\text{CO})_x^+$  species are complex. It should be realized that this is a general problem for all CID reactions (even though the ligand exchange product is often not collected) because the ligand exchange process will always have a lower threshold than CID, no matter what neutral reagent is used. As discussed in detail elsewhere,<sup>8</sup> we do not believe that this competition is likely to affect our measurements. Conservatively, the bond energies measured here and in any CID study constitute upper limits to the adiabatic BDEs under investigation (assuming that energy broadening effects are adequately compensated for and the data are analyzed over an extensive energy and magnitude range); however, previous experience suggests that such CID values are likely to be accurate measures of the true bond energies.

**Ligand-Exchange Reaction.** Analysis of the cross section for the ligand exchange reaction 4 in the  $\text{CoCO}^+$  system, Figure 2, leads to a threshold of  $1.00 \pm 0.12$  eV, Table 4. The BDE of  $\text{CoXe}^+$  can be determined from the difference between this threshold energy and the threshold we measure for the reaction of  $\text{CoCO}^+ + \text{Xe}$  to form  $\text{Co}^+ + \text{CO} + \text{Xe}$ . This gives a value for  $D_0(\text{Co}^+-\text{Xe})$  of  $0.80 \pm 0.14$  eV, in good agreement with the previously determined value of  $D_0(\text{Co}^+-\text{Xe}) = 0.85 \pm 0.07$  eV.<sup>36</sup>

## Discussion

**Comparison with Literature Thermochemistry.** Probably the best measure of the accuracy of the thermochemistry derived here is to compare the sum of the four cobalt-carbonyl bond energies we measure with that calculated from the heat of formation of  $\text{Co}(\text{CO})_4^+$ , Table 2. As discussed above, the heat of formation in the literature leads to a bond energy sum of  $5.11 \pm 0.17$  eV at 0 K. In our studies, the sum of these four 0 K bond energies is  $4.98 \pm 0.17$  eV if we use the vibrational frequencies for a square planar  $\text{Co}(\text{CO})_4^+$  complex ( $5.04 \pm 0.18$  eV if frequencies for a tetrahedral complex are used). Either of these is in excellent agreement with the literature value and hence our final value for  $D_0[(\text{CO})_3\text{Co}^+-\text{CO}]$ ,  $0.78 \pm 0.06$  eV,

is the average of the values obtained with the two sets of frequencies in Table 3.

If we use the sum of our BDE values,  $5.01 \pm 0.18$  eV, combined with the well known heats of formation of  $\text{Co}^+$  and  $\text{CO}$ , Table 2, we derive the heat of formation for  $\text{Co}(\text{CO})_4^+$  at 0 K as  $245 \pm 18$  kJ/mol ( $256 \pm 18$  kJ/mol at 298 K), a value that is independent of any previously determined thermochemistry for this species. Combined with  $\text{IE}[\text{Co}(\text{CO})_4] = 8.3 \pm 0.1$  eV,<sup>10</sup> this yields  $\Delta_f H_0^\circ[\text{Co}(\text{CO})_4] = -556 \pm 20$  kJ/mol and  $\Delta_f H_{298}^\circ[\text{Co}(\text{CO})_4] = -551 \pm 20$  kJ/mol, in excellent agreement with the  $-561 \pm 12$  kJ/mol value used by Pilcher and Skinner,<sup>22,23</sup> Connor,<sup>24</sup> and Simoes and Beauchamp.<sup>25</sup> Combined with  $\Delta_f H_{298}^\circ[\text{Co}_2(\text{CO})_8]$ , Table 2, this heat of formation leads to  $D_{298}[(\text{CO})_4\text{Co}-\text{Co}(\text{CO})_4] = 83 \pm 29$  kJ/mol. This is within experimental error of the 298 K value of Bidinosti and McIntyre<sup>10,11</sup> ( $61 \pm 8$  kJ/mol) and in good agreement with the values cited by Simoes and Beauchamp<sup>25</sup> (64 kJ/mol), Connor<sup>24</sup> (68 kJ/mol), Pilcher<sup>23</sup> (92 kJ/mol), and Skinner and Pilcher<sup>22</sup> (87.8 kJ/mol). It is much lower than the value of 318 kJ/mol provided by Winters and Kiser,<sup>9</sup> or the revised value of  $578 \pm 56$  kJ/mol, and lower than the 148 kJ/mol theoretical value of Folga and Ziegler.<sup>26</sup>

Comparison of the individual BDEs measured here to values obtained from electron impact appearance energies is given in Table 1. In all cases, the present values are reasonably consistent with the *lowest* of these values. This can be explained by kinetic shifts in the AE thresholds and the difficulty in assigning accurate AE values to ion yield curves that rise slowly from the thermodynamic thresholds.

Our value for  $D_0[\text{Co}^+-\text{CO}]$  is much higher than that obtained by Hanratty et al.<sup>18</sup> in their KERD experiment on  $\text{Co}^+(\text{acetone-}d_6)$  eliminating ethane- $d_6$ , but in good agreement with the value obtained in a reanalysis of these data by Carpenter et al.<sup>19</sup> The discrepancy between these BDEs is explained by angular momentum constraints along the reaction path remote from the final transition state,<sup>37</sup> a factor that was not included in the initial analysis.

Finally, we compare our BDE values for the mono- and dicarbonyl to results of ab initio calculations performed by Barnes et al.<sup>20</sup> With relativistic corrections, they obtained  $D_e[\text{Co}^+-\text{CO}] = 1.62$  eV and  $D_e[(\text{CO})\text{Co}^+-\text{CO}] = 1.40$  eV, which can be converted to 0 K values of 1.55 and 1.31 eV, respectively, based on the vibrational frequencies in Table 3. These values are substantially lower than our results, although the difference between the first and second BDEs, 0.24 eV, is comparable to our experimental difference of 0.22 eV. The discrepancy is somewhat surprising because the ab initio calculations for the mono- and dicarbonyl cations of chromium and iron showed reasonable agreement with our experimentally determined values.<sup>4,5</sup> However, comparable discrepancies between our experiments and these theoretical results have been obtained for the nickel,<sup>6</sup> copper, and silver<sup>38</sup> mono- and dicarbonyl cation bond energies. More recent calculations<sup>39</sup> of the  $\text{Ag}(\text{CO})^+$  and  $\text{Ag}(\text{CO})_2^+$  thermochemistry are in excellent agreement with the results of our studies, suggesting that the discrepancies noted here are largely because of inadequacies in the calculations of Barnes et al.<sup>20</sup> This appears to be because  $\pi$ -back-bonding

(34) Armentrout, P. B.; Simons, J. *J. Am. Chem. Soc.* **1992**, *114*, 8627.

(35) Dearden, D. V.; Hayashibara, K.; Beauchamp, J. L.; Kirchner, N. J.; van Koppen, P. A. M.; Bowers, M. T. *J. Am. Chem. Soc.* **1989**, *111*, 2401.

(36) Haynes, C. L.; Armentrout, P. B.; Perry, J. K.; Goddard, W. A., III *J. Phys. Chem.* **1995**, *99*, 6340.

(37) van Koppen, P. A. M.; Brodbelt-Lustig, J.; Bowers, M. T.; Dearden, D. V.; Beauchamp, J. L.; Fisher, E. R.; Armentrout, P. B. *J. Am. Chem. Soc.* **1990**, *112*, 5663. van Koppen, P. A. M.; Brodbelt-Lustig, J.; Bowers, M. T.; Dearden, D. V.; Beauchamp, J. L.; Fisher, E. R.; Armentrout, P. B. *J. Am. Chem. Soc.* **1991**, *113*, 2359.

(38) Meyer, F.; Armentrout, P. B. *J. Am. Chem. Soc.* **1995**, *117*, 4071.

(39) Veldkamp, A.; Frenking, G. *Organometallics* **1993**, *12*, 4613.

**Table 5.** Likely Structures and Spin States of  $\text{Co}(\text{CO})_x^+$  ( $x = 1-5$ ) Complexes

complex	structure	symmetry	ground state
$\text{CoCO}^+$ <sup>a</sup>	linear	$C_{\infty v}$	$^3\Delta$
$\text{Co}(\text{CO})_2^+$ <sup>a</sup>	linear	$D_{\infty h}$	$^3\Delta_g$
$\text{Co}(\text{CO})_3^+$	trigonal planar	$D_{3h}$	$^3A_2$
$\text{Co}(\text{CO})_4^+$	square planar	$D_{4h}$	$^3B_{2g}, ^1A_{1g}$
$\text{Co}(\text{CO})_5^+$	trigonal bipyramid	$D_{3h}$	$^1A_{1g}$
	square pyramid	$C_{4v}$	$^1A_1$

<sup>a</sup> Reference 20.

contributions to the bonding have been underestimated in the calculations.<sup>40</sup>

**Electronic and Geometric Structures of  $\text{Co}(\text{CO})_x^+$ .** To further understand the dissociation behavior and energetics observed here, it would be advantageous to know the ground electronic states and structures of the  $\text{Co}(\text{CO})_x^+$  ( $x = 1-5$ ) complex ions. The structures of the first two complexes,  $x = 1-2$ , have been calculated to be linear with  $^3\Delta$  and  $^3\Delta_g$  ground states, respectively.<sup>20</sup> No calculations have been performed on the  $x = 3-5$  species, so we estimate their properties by using the extended Huckel calculations carried out on  $\text{M}(\text{CO})_x$  systems by Elian and Hoffmann.<sup>41</sup> This work computes the energies of metal d orbitals as the number of d electrons and geometry of  $\text{M}(\text{CO})_x$  are varied. In order to predict the ground states of these species, we also need to know the exchange energy lost upon pairing electrons. We take the triplet-singlet pairing energy to be 1.44 eV (the difference in energy between the  $^3F$  and  $^1D$  states of  $\text{Co}^+$ ).<sup>42</sup>

For the  $\text{Co}(\text{CO})_3^+$  complex, the orbital energy diagrams suggest that the lowest energy structure is probably the  $D_{3h}$  symmetry trigonal planar geometry with a triplet spin, although distortions to nonplanar structures do not appear to increase the energy very much. The valence electron configuration on the metal is  $e^4a_1^2e''^2$ , such that the ground state is  $^3A_2$  and any singlet state must lie above the triplet ground state by approximately the spin pairing energy.

For the  $\text{Co}(\text{CO})_4^+$  complex, the lowest energy structure appears to be the  $D_{4h}$  square planar geometry. The  $^3A_{2u}$  state with a  $b_{2g}^2e_g^4a_{1g}^1a_{2u}^1$  valence electron configuration and  $^1A_{1g}$  ( $b_{2g}^2e_g^4a_{1g}^2$ ) state are comparable in energy with the former about 0.2 eV lower (although the assignment of the ground state cannot be made confidently on the basis of these Huckel diagrams). Nonplanar  $D_{2d}$  (toward tetrahedral),  $C_{4v}$  (toward square pyramid), and  $C_{2v}$  (toward a sawhorse geometry) distortions are energetically unfavorable. The tetrahedral complex is estimated to lie about 1.6 eV higher in energy for the triplet state and about 2.5 eV higher for the singlet state.

For the  $\text{Co}(\text{CO})_5^+$  complex, the orbital energies clearly indicate that the complex has a singlet spin with a triplet state much higher in energy. The  $D_{3h}$  symmetry trigonal bipyramid and the  $C_{4v}$  symmetry square planar geometries have comparable energies, so we imagine the former is likely to be the ground state in analogy with the isoelectronic  $\text{Fe}(\text{CO})_5$  species. The valence electron configurations are  $e''^4e^4$  leading to a  $^1A_1'$  state and  $b_2^2e^4a_1^2$  leading to a  $^1A_1$  state, respectively. The electronic and physical structures resulting from these considerations are summarized in Table 5.

A key conclusion that can be drawn from the electronic states suggested here for the  $\text{Co}(\text{CO})_x^+$  complexes is that all the dissociations examined here are spin-allowed for ground state complexes to form ground state products, except for  $\text{Co}(\text{CO})_5^+$

if  $\text{Co}(\text{CO})_4^+$  has a triplet ground state or for  $\text{Co}(\text{CO})_4^+$  if it has a singlet ground state. In either of these cases, the threshold measured here for dissociation of  $\text{Co}(\text{CO})_4^+$  must correspond to formation of ground state triplet  $\text{Co}(\text{CO})_3^+$ . If  $\text{Co}(\text{CO})_4^+$  is a ground state triplet, then this dissociation path is the spin-allowed adiabatic dissociation channel. If  $\text{Co}(\text{CO})_4^+$  is a ground state singlet and its dissociation occurred along the spin-allowed path to form singlet  $\text{Co}(\text{CO})_3^+$ , which is estimated to lie about 1.4 eV higher than the ground state triplet (see above), then our sum of bond energies for  $x = 1-4$  would disagree with the literature.

If  $\text{Co}(\text{CO})_4^+$  has a triplet ground state, then dissociation of singlet  $\text{Co}(\text{CO})_5^+$  could occur via the adiabatic but spin-forbidden pathway or along the spin-allowed path to form excited  $\text{Co}(\text{CO})_4^+$ . If the excitation energy is truly on the order of 0.2 eV, as estimated above, then the distinction between these pathways will not be obvious in the threshold measured nor will the thermochemical results in Table 1 change appreciably. It is most likely that the  $\text{Co}(\text{CO})_5^+$  dissociation would correspond to the adiabatic process, as appears to be the case for several other metal carbonyl cation systems in which spin-changes also occur.<sup>4,5</sup>

**Trends in Sequential Bond Energies of  $\text{Co}(\text{CO})_x^+$ .** In two related systems studied recently in this laboratory,  $\text{Fe}(\text{CO})_x^+$  and  $\text{Cr}(\text{CO})_x^+$ ,<sup>4,5</sup> the sequential BDEs vary *nonmonotonically*. We have suggested that some of these variations can probably be explained in terms of changes in spin that occur when CO molecules are added to high-spin metal ions to form low-spin  $\text{Fe}(\text{CO})_5^+$  and  $\text{Cr}(\text{CO})_6^+$  complexes. In contrast to these systems, the  $\text{Co}(\text{CO})_x^+$  system shows strictly *monotonic* behavior, similar to our observations for the  $\text{Ni}(\text{CO})_x^+$  system.<sup>6</sup> Such monotonic behavior in the sequential BDEs might be expected on the basis of electrostatic considerations. As the number of CO ligands increases around the metal ion, so do the ligand-ligand repulsions, thus weakening the bonds. For  $\text{Ni}(\text{CO})_x^+$ , this explanation seems reasonable because there are no spin changes occurring from  $\text{Ni}^+$ , which has a  $^2D$  ground state, to  $\text{Ni}(\text{CO})_4^+$ , which also must have a doublet ground state as a single electron is removed from the 18-electron  $\text{Ni}(\text{CO})_4$  complex.

The situation is different for  $\text{Co}(\text{CO})_x^+$ . As discussed above, it seems very likely that the pentacarbonyl has a singlet ground state and the spin change from triplet to singlet probably occurs upon addition of either the fourth or fifth CO ligand. In considering whether the sequential bond energies measured here reveal where this spin change occurs, it is useful to compare with other metal ligand complexes. Initially, we compare with the weak field ligand,  $\text{H}_2$ , because it and CO are both  $\sigma$ -donating and  $\pi$ -accepting ligands. Kemper et al. have measured the sequential binding energies of one to seven  $\text{H}_2$  molecules to  $\text{Co}^+$ .<sup>43</sup> As shown in Figure 7, the first two  $\text{H}_2$  bond energies are similar, then decrease for the third and fourth ligands, and then decrease again for the fifth and sixth ligands. The pattern parallels that for  $D_0[(\text{CO})_{x-1}\text{Co}^+-\text{CO}]$  measured here for  $x = 1-4$ , such that the latter values average  $2.1 \pm 0.2$  times greater than  $D_0[(\text{H}_2)_{x-1}\text{Co}^+-\text{H}_2]$ . However, rather than see a decrease for the fifth CO ligand, as observed for the fifth  $\text{H}_2$ , we find that the carbonyl bond energy remains fairly constant. This can be rationalized by the spin change, as a singlet state has fewer electrons in the antibonding orbitals of the complex, thereby allowing a stronger bond. No spin change is anticipated for the weaker field  $\text{H}_2$  ligand. Although this argument plausibly shows that  $\text{Co}(\text{CO})_5^+$  has a singlet ground state, it still does

(40) Bauschlicher, C. W., Jr. Personal communication.

(41) Elian, M.; Hoffmann, R. *Inorg. Chem.* **1975**, *14*, 1058.(42) Sugar, J.; Corliss, C. *J. Phys. Chem. Ref. Data* **1985**, *14*, Suppl. No. 2.(43) Kemper, P. R.; Bushnell, J.; von Helden, G.; Bowers, M. T. *J. Phys. Chem.* **1993**, *97*, 52.

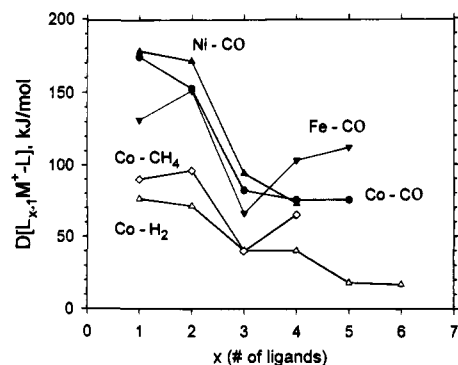


**Figure 7.** Comparison of transition metal–ligand bond strengths for  $\text{Fe}(\text{CO})_x^+$  ( $x = 1-5$ ) (ref 4),  $\text{Co}(\text{CO})_x^+$  ( $x = 1-5$ ) (this study),  $\text{Ni}(\text{CO})_x^+$  ( $x = 1-4$ ) (ref 6),  $\text{Co}(\text{CH}_4)_x^+$  ( $x = 1-4$ ) (ref 36), and  $\text{Co}(\text{H}_2)_x^+$  ( $x = 1-6$ ) (ref 43) versus  $x$ .

not definitively demonstrate whether  $\text{Co}(\text{CO})_4^+$  has a singlet ground or low-lying excited state, as either could explain the sequential bond energies observed here.

While the comparison of the  $\text{Co}(\text{CO})_x^+$  BDEs to those for  $\text{Ni}(\text{CO})_4^+$  and  $\text{Co}(\text{H}_2)_x^+$  provides a useful picture of the bonding, additional comparisons to other complexes demonstrate that our understanding of such sequential bond energies is still in its infancy. Also shown in Figure 7 are the bond energies for  $\text{Co}(\text{CH}_4)_x^+$  and  $\text{Fe}(\text{CO})_x^+$  taken from our work.<sup>4,36</sup> The former are in good agreement with measurements for  $x = 1-3$  by Kemper et al.<sup>44</sup> and calculated by Perry et al.<sup>36,45</sup> There is still some disagreement over the precise values for the  $\text{Fe}(\text{CO})_x^+$  bond energies, as discussed elsewhere,<sup>4,27</sup> but our values are representative of the trends. It can be seen from Figure 7 that the pattern in the  $\text{Co}(\text{CH}_4)_x^+$  bond energies differs from those for  $\text{Co}(\text{H}_2)_x^+$  and  $\text{Co}(\text{CO})_x^+$ . The second bond is slightly stronger than the first and the fourth is appreciably stronger than the third. These trends have been attributed largely to effects of  $sd$  hybridization, as discussed in detail elsewhere.<sup>36</sup> Briefly, this argument contends that the first ligand induces  $s-d\sigma$  hybridization to remove electron density from the metal–ligand axis, thereby allowing a shorter bond length and enhancement of the electrostatic bonding. As this hybridization removes electron density along this axis on both sides of the metal, the second ligand can bind more strongly without paying the promotion energy costs associated with the hybridization. A third ligand can no longer take advantage of this situation and hence the bond energy is substantially weaker. The fourth bond can be stronger because the third ligand has already paid the energetic cost associated with destroying the  $sd$  hybridization. Ricca and Bauschlicher make similar arguments to explain the bond energies of  $\text{Fe}(\text{CO})_x^+$  ( $x = 1-4$ ).<sup>27</sup> [Here it should be noted that the first  $\text{Fe}^+-\text{CO}$  bond energy is particularly weak because a spin change occurs for the adiabatic dissociation of  $\text{FeCO}^+(\text{^4}\Sigma^-)$  to  $\text{Fe}^+(\text{^6}\text{D})$ . To remove this, the promotion energy to the  $\text{Fe}^+(\text{^4}\text{F})$  state,  $0.23 \text{ eV} = 22 \text{ kJ/mol}$ , can be added to this bond energy.] Ricca and Bauschlicher find that there are both low- and high-spin states of  $\text{Fe}(\text{CO})_4^+$  that are comparable in energy, similar to the situation we predict above for  $\text{Co}(\text{CO})_4^+$ , and that  $\text{Fe}(\text{CO})_5^+$  has a low-spin ground state, as we suggest above for  $\text{Co}(\text{CO})_5^+$ .

The comparisons with these complexes suggest that the large drops seen in the BDEs for the third ligand in all the complexes shown in Figure 7 are primarily due to the loss of  $sd$  hybridization. For all of these complexes, the first two ligand

bond energies are enhanced because  $s-d\sigma$  hybridization removes electron density along the metal–ligand axis. However, if this is true, then why is the fourth bond energy greater than the third in two cases and weaker in several others? One consideration comes from work of Bauschlicher and Maitre on the  $\text{Co}(\text{H}_2)_x^+$  ( $x = 1-6$ ) clusters.<sup>46</sup> They calculated that the  $sd$  hybridization is not lost completely until  $x = 5$ . Some hybridization is maintained for  $x = 3$  and 4 clusters by mixing  $4p$  character into the  $4s-3d\sigma$  hybrid orbital, thereby allowing it to polarize away from the third and fourth hydrogen ligands. Such an effect could also occur for  $\text{Co}(\text{CO})_x^+$  and  $\text{Ni}(\text{CO})_x^+$  clusters (systems where the fourth BDE is comparable to the third) but not for  $\text{Co}(\text{CH}_4)_x^+$  and  $\text{Fe}(\text{CO})_x^+$ . The question now is why this polarization does not occur for the latter two complexes. If we concentrate just on the carbonyl systems, the distinct behavior of  $\text{Fe}(\text{CO})_x^+$  is presumably because  $\text{Fe}^+$  has fewer electrons than  $\text{Co}^+$  and  $\text{Ni}^+$ . Because this electron is removed from an antibonding orbital for  $x = 4$  and 5, the bond energies for  $\text{Fe}(\text{CO})_4^+$  and  $\text{Fe}(\text{CO})_5^+$  can be greater than for the  $\text{Co}$  and  $\text{Ni}$  analogues. Comparison of the three cobalt complexes suggests that the distinct behavior of  $\text{Co}(\text{CH}_4)_x^+$  is because  $\text{CH}_4$  is a weak  $\sigma$ -donating and  $\pi$ -donating ligand, rather than a  $\pi$ -accepting ligand as with  $\text{CO}$  and  $\text{H}_2$ . This drastically reorganizes the molecular orbitals by destabilizing the  $\pi$  orbitals on the metal. This effect can be seen clearly by comparing Figures 5 (for tetracoordinate fragments with  $\text{CO}$  ligands) and 10 (for tetracoordinate fragments with  $\text{Cl}$  ligands) in the Elian and Hoffmann paper.<sup>41</sup> In this case, it could be argued that the strong  $\pi$ -back-bonding in  $\text{Co}(\text{CO})_x^+$  can overshadow the  $sd$  hybridization effect and allow the  $4p$  polarization, while in  $\text{Co}(\text{CH}_4)_x^+$ , the more electrostatic bonding allows the  $sd$  hybridization to play a more prominent role. However, the former seems likely to be true for  $\text{Fe}(\text{CO})_x^+$  as well, but here the difference in the number of  $d$  electrons plays a role, as noted above.

**Comparison with Isolelectronic Species.** There are a large number of experimental<sup>47-51</sup> and theoretical<sup>52-55</sup> studies concerning the bond energies of neutral  $\text{Fe}(\text{CO})_x$  species, isoelectronic with the  $\text{Co}(\text{CO})_x^+$  complexes examined here. In general, the agreement among these studies is poor. Recent theoretical numbers for  $\text{Fe}(\text{CO})_x$  ( $x = 1-5$ ) from Barnes, Rosi, and Bauschlicher (BRB) are listed in Table 6,<sup>53</sup> although these values are known to be too low as the sum of the bond energies is only 77% of the value calculated from the heat of formation of  $\text{Fe}(\text{CO})_5$ .<sup>4</sup> A complete set of  $\text{Fe}(\text{CO})_x$  BDEs can be derived from two pairs of experiments. The first, listed in Table 6, combines appearance energy measurements for  $\text{Fe}(\text{CO})_x^-$  from Compton and Stockdale (CS)<sup>56</sup> with electron affinity (EA) measurements of Engelking and Lineberger (EL).<sup>51</sup> A more reliable set of numbers is obtained by combining these EA

(46) Bauschlicher, C. W., Jr.; Maitre, P. *J. Phys. Chem.* **1995**, *99*, 3444.

(47) Lewis, K. E.; Golden, D. M.; Smith, G. P. *J. Am. Chem. Soc.* **1984**, *106*, 3905.

(48) Sunderlin, L. S.; Wang, D.; Squires, R. R. *J. Am. Chem. Soc.* **1992**, *114*, 2788.

(49) Siefert, E. E.; Angelici, R. *J. Organomet. Chem.* **1967**, *8*, 374.

(50) Venkataraman, B. K.; Bandukwalla, G.; Zhang, Z.; Vernon, M. *J. Chem. Phys.* **1989**, *90*, 5510.

(51) Engelking, P. C.; Lineberger, W. C. *J. Am. Chem. Soc.* **1979**, *101*, 5569.

(52) Ziegler, T.; Tschinke, V.; Ursenbach, C. *J. Am. Chem. Soc.* **1987**, *109*, 4825.

(53) Barnes, L. A.; Rosi, M.; Bauschlicher, C. W. *J. Chem. Phys.* **1991**, *94*, 2031.

(54) Bauschlicher, C. W.; Bagus, P. S.; Nelin, C. J.; Roos, B. O. *J. Chem. Phys.* **1986**, *85*, 354.

(55) Bauschlicher, C. W.; Bagus, P. S. *J. Chem. Phys.* **1984**, *81*, 5889.

(56) Compton, R. N.; Stockdale, J. A. D. *Int. J. Mass Spectrom. Ion Phys.* **1976**, *22*, 47.

(44) Kemper, P. R.; Bushnell, J.; van Koppen, P.; Bowers, M. T. *J. Phys. Chem.* **1993**, *97*, 1810.

(45) Perry, J. K.; Ohanessian, G.; Goddard, W. A., III *J. Phys. Chem.* **1993**, *97*, 5238.



**Table 6.** Summary of 0 K Adiabatic Values for  $D_0[(\text{CO})_{x-1}\text{M}-\text{CO}]$  (kJ/mol)<sup>a</sup>

species	$x = 1$	$x = 2$	$x = 3$	$x = 4$	$x = 5$	source
M = Co <sup>+</sup>	174(7)	152(3)	82(12)	75(6)	75(5)	this work
M = Fe	96(29)	96(29)	135(29)	19(39)	232(48)	exp, CS-EL <sup>b</sup>
	34(15)	154(15)	122(24)	117(37)	174(8) <sup>c</sup> [106(8)] <sup>d</sup>	exp, SWS-EL <sup>e</sup>
	>21	92	105	130	163 [95] <sup>d</sup>	theory, BRB <sup>f</sup>
M = Mn <sup>-</sup>			120(13)	174(13)	193(13)	exp, SWS <sup>g</sup>

<sup>a</sup> Uncertainties are reported in parentheses. <sup>b</sup> References 51 and 56. <sup>c</sup> Reference 47. <sup>d</sup> Value corrected to an adiabatic BDE by using the excitation energy of Fe(CO)<sub>4</sub> calculated in ref 53. <sup>e</sup> References 48 and 51. <sup>f</sup> Reference 53. <sup>g</sup> Reference 57.

values with BDEs for Fe(CO)<sub>x</sub><sup>-</sup> ( $x = 1-4$ ) measured by Sunderlin, Wang, and Squires (SWS) using CID methods.<sup>48</sup> This yields values for  $D_{298}[(\text{CO})_{x-1}\text{Fe}-\text{CO}]$  ( $x = 1-4$ ), which are listed in Table 6. Reasonable agreement between the two sets of experimental values and theoretical values of BRB<sup>53</sup> is obtained only for  $x = 3$ . For  $x = 1$  and 4, theory agrees with the SWS-EL BDEs, while it agrees with the CS-EL values for  $x = 2$ .  $D_{298}[(\text{CO})_4\text{Fe}-\text{CO}]$  is taken from the gas-phase pulsed laser pyrolysis study of Lewis, Golden, and Smith,<sup>47</sup> but it seems likely that their dissociation energy of  $174 \pm 8$  kJ/mol corresponds to the spin-allowed dissociation to an excited singlet state of Fe(CO)<sub>4</sub> based on the theoretical value for this dissociation of 163 kJ/mol.<sup>53</sup> This BDE is corrected to an adiabatic value based on the Fe(CO)<sub>4</sub> excitation energy of 68 kJ/mol calculated by Barnes et al.<sup>53</sup>

Also listed in Table 6 are the bond energies for the isoelectronic manganese carbonyl anions, Mn(CO)<sub>x</sub><sup>-</sup> ( $x = 3-5$ ), also measured by SWS.<sup>57</sup> In cases where BDEs for all three metal systems are known ( $x = 3-5$ ), the bond energies follow the ordering  $D[(\text{CO})_{x-1}\text{Mn}^--\text{CO}] \geq D[(\text{CO})_{x-1}\text{Fe}-\text{CO}] \geq D[(\text{CO})_{x-1}\text{Co}^+-\text{CO}]$ . This trend has been noted in an analogous series by SWS<sup>57</sup> and can be rationalized as a difference in  $\pi$  back-bonding ability of corresponding complexes with differing metal nuclear charges. This trend clearly shows that electrostatic effects do not dominate the bond energies.

The total binding energies of Fe(CO)<sub>5</sub> and Co(CO)<sub>5</sub><sup>+</sup> are comparable,  $572 \pm 7^{58}$  and  $559 \pm 18$  kJ/mol, respectively. The sequential BDEs of  $D[\text{M}-\text{CO}]$ ,  $D[(\text{CO})\text{M}-\text{CO}]$ ,  $D[(\text{CO})_2\text{M}-\text{CO}]$ ,  $D[(\text{CO})_3\text{M}-\text{CO}]$ , and  $D[(\text{CO})_4\text{M}-\text{CO}]$  for M = Co<sup>+</sup> constitute percentages of the total binding energy of 31, 27, 15, 13, and 13%, respectively. The theoretical values for M = Fe are >5, 21, 24, 29, and 21%, respectively, and the SWS-EL values for M = Fe are 6, 29, 23, 22, and 20%, respectively. As noted above, the trends in the BDEs for addition of the first several CO ligand to Co<sup>+</sup> can be rationalized largely on the basis of  $s-d\sigma$  hybridization at the metal center because there are no promotion energy effects or spin changes. In contrast, promotion is necessary in the Fe system because the ground state of Fe is <sup>5</sup>D(4s<sup>2</sup>3d<sup>6</sup>), while the Fe(CO)<sub>x</sub> ( $x = 1-4$ ) species

are believed to have triplet ground states.<sup>59,60</sup> Such a promotion energy effect clearly explains why the first carbonyl bond to Co<sup>+</sup> is much larger than that to Fe, which must be promoted to its lowest triplet state, <sup>3</sup>F(4s3d<sup>7</sup>), lying 1.48 eV above the ground state.<sup>42</sup>

In the Fe(CO)<sub>x</sub> ( $x = 1-5$ ) system, it is known experimentally that a spin change from triplet to singlet takes place going from  $x = 4$  to 5.<sup>61</sup> For both the theoretical and experimental BDEs, the spin-allowed BDE of Fe(CO)<sub>5</sub> is much higher than those for Fe(CO)<sub>x</sub> ( $x = 3$  and 4), Table 6, while the adiabatic BDE is comparable to these others. Given our observation that  $D_0[(\text{CO})_{x-1}\text{Co}^+-\text{CO}]$  are comparable for  $x = 3-5$ , this is consistent with our assignment that the spin-change from triplet to singlet probably occurs between  $x = 4$  and 5 rather than between  $x = 3$  and 4.

## Conclusions

We report systematic measurements of the collision-induced dissociation (CID) of Co(CO)<sub>x</sub><sup>+</sup> ( $x = 1-5$ ) ions with Xe by using guided-ion beam mass spectrometry. From the thresholds for these processes and ligand exchange, bond dissociation energies at 0 K are determined for CoXe<sup>+</sup>, (CO)<sub>4</sub>Co<sup>+</sup>-CO, (CO)<sub>3</sub>Co<sup>+</sup>-CO, (CO)<sub>2</sub>Co<sup>+</sup>-CO, (CO)Co<sup>+</sup>-CO and Co<sup>+</sup>-CO. This method avoids possible errors due to kinetic shifts that plague measurements of this thermochemistry in electron impact appearance energy experiments. The sum of the last four of these values is in good agreement with literature thermochemistry, as is the CoXe<sup>+</sup> BDE. Combined with  $\text{IE}[\text{Co}(\text{CO})_4] = 8.3 \pm 0.1$  eV,<sup>10</sup> the present results yield  $\Delta_f H_{298}^\circ[\text{Co}(\text{CO})_4] = -551 \pm 20$  kJ/mol and  $D_{298}[(\text{CO})_4\text{Co}-\text{Co}(\text{CO})_4] = 83 \pm 29$  kJ/mol. Trends in the sequential bond energies of Co(CO)<sub>x</sub><sup>+</sup> ( $x = 1-5$ ) are discussed and compared with the trends for several other metal complexes.

**Acknowledgment.** This work is supported by the National Science Foundation, Grant No. CHE-9221241. S.G. thanks the German Academic Exchange Service (DAAD) for providing a scholarship to enable the participation in this research project.

JA950822+

(59) Howard, I. A.; Pratt, G. W.; Johnson, K. H.; Dresselhaus, G. *J. Chem. Phys.* **1981**, *74*, 3415.

(60) Villalta, P. W.; Leopold, D. G. *J. Chem. Phys.* **1993**, *98*, 7730.

(61) Poliakov, M.; Turner, J. J. *J. Chem. Soc., Dalton Trans.* **1974**, *70*, 93.

(57) Sunderlin, L. S.; Wang, D.; Squires, R. R. *J. Am. Chem. Soc.* **1993**, *115*, 12060.

(58) Thermochemistry for Fe(CO)<sub>5</sub> is summarized in ref 4.